Uranium distribution in the Upper Cretaceous-Tertiary Belqa Group, Yarmouk Valley, northwest Jordan

Basem K. Moh'd[1*] and John H. Powell[2]

1. Civil Engineering Department, Tafila Technical University (TTU), Tafila, Jordan
2. British Geological Survey, Nottingham, NG12 5RA UK

* Corresponding author

Abstract

Uranium distribution has been studied in the outcropping Upper Cretaceous-Tertiary rocks (Belqa Group) in northwest Jordan. Representative samples of phosphorite, chert, silicified limestone, chalk, marl, fossiliferous limestone and glauconitic limestone were collected and chemically analyzed using XRF techniques. Uranium values range between less than 1 ppm and 70 ppm. The highest U concentration (52-70 ppm) was encountered in the phosphatic rocks. Uranium values in other lithologies are up to 19 ppm. The lowest values were encountered in fossiliferous limestone (<1 ppm), chert (2 ppm), silicified limestone, almost pure chalk and silicified chalk (4 ppm). Uranium concentrations in northwest Jordanian chalks are higher than Cretaceous chalks of the USA and Europe (North Sea). Uranium is positively related with P_2O_5 (francolite in phosphorite). Organic matter could be related to elevated levels of uranium in highly bituminous marl (average of 25 ppm). Uranium is positively associated with Cr, Zn, Mo, As, Sc and V (correlation coefficients r> 0.80). When U is cross-plotted against other variables, aggregation based on lithology became clear and the importance of other factors (with r>0.80) such as alumina, total iron oxides, P_2O_5, LOI (loss on ignition) Ni, Cl, As, Mo, Cd, La became evident. Factor analysis showed that uranium is distributed in clay and carbonates, depositional groundwater and organic matter, and phosphorite. Weak loadings are observed with factor 2 in comparison to factors 1 and 3.
Uranium concentrations in Jordanian and similar chalks can be predicted from the knowledge of alumina, total iron oxides, P_2O_5, and LOI.

Introduction

Jordan faces two main challenges: lack of conventional energy resources and scarcity of water. The increasing cost of oil and gas imports, that currently supply most of the country's energy needs, severely affects its economic growth and security of supply. Hence, the development of a secure alternative energy supply is a top priority for Jordan. Jordan established the Jordan Atomic Energy Commission (JAEC), early in 2008, to lead the national efforts and implement Jordan's nuclear energy program. Dr. Khaled Toukan, the chairman of the Jordan Atomic Energy Commission, announced in an invited talk to the Symposium on the Technology of Peaceful Nuclear Energy, Yarmouk University-Jordan (Oct. 14-16, 2008) that 'following assessment of exploration and extraction of the proven uranium ore reserves, including domestic phosphate deposits, Jordan will sign mining agreements later this year, and we expect uranium production to begin by 2012. Jordan's plan is to generate electric power from its nuclear power reactors by 2016 and to export electricity by 2030'.

Uranium and its natural series radionuclides Th, ^{226}Ra and ^{222}Rn are widely distributed in a number of geological settings in Jordan. Uranium occurrences in phosphorite, oil shale (bituminous limestone), limestone, marble, sandstones, and thermal waters of Jordan were studied by many workers mainly during regional mapping and mineral exploration projects (Abu Ajamieh, 1974, 1981, 1987; Phoenix Corp., 1980; Abed and Khalid, 1985; Abu Ajamieh et al, 1988; Helmdach et al, 1985; Healy and Young, 1998; Wriekat et al, 1987; NRA, 1997; Smith et al., 1996a, b). The present work aims at examining the association of uranium with major, minor, and other trace elements in the chalk-dominated Belqa Group succession in northwest Jordan. It includes a comparison of uranium content with similar chalk-dominated successions worldwide, including 'average' limestone, and regional phosphate, oil shale and marble occurrences. In addition, geochemical proxies useful for uranium exploration are suggested.

Groundwater pollution by natural radionuclides has been reported from local aquifers in the Amman area (Smith et al., 1996a,b); the source of the radiological hazard ^{222}Rn and elevated levels of uranium exceeding 1 mg/l is thought not to be from primary leaching of U from phosphorite deposits, but the result of carbonate groundwater mixing, at depth, with uranium mineralization of Cretaceous aquifers (Ajlun Group; Table 1) along the Amman-Hallabat fault (Smith et al.,1995). In addition, high levels of uranium have been reported form Late Cretaceous to Neogene phosphorites (Abed and Khaled, 1985). Other uraniferous geological terranes are the Ordovician-Silurian marine sandstones and mudstones of the southern Desert (Abu Ajamieh et al., 1988) and Late Cretaceous to Palaeogene oil shales (oil-saturated marls) (Abu Ajamieh, 1981, 1988; Wriekat et al., 1987).

High levels of U, Th, ^{226}Ra and ^{222}Rn have also been reported elsewhere in the Mediterranean Basin from groundwaters derived from middle Miocene age carbonate-gypsum aquifers (Discospirina beds) of the Maroni region, Cyprus (Smith et al., 1997).

Geological Setting

The study area (Figure 1), situated 90 km north-northwest of Amman, was mapped at 1: 50 000 scale (Moh'd, 2000). The lithostratigraphy and lithology of the Late Cretaceous to Tertiary (Neogene) succession of the area is presented in Table 1 (after Powell, 1989). Superficial deposits, comprising calcrete, travertine, alluvium, alluvial fans and soil, are also present. The sampled rock units are briefly described here after Moh'd (2000).

The **Maestrichtian Al-Hisa Phosphorite Formation** is 10-15 m thick and consists of phosphate, phosphatic chert, limestone, coquina and marl. Mega-fossils include the ammonite *Baculites* and bivalves. There are 16 species and subspecies of the microfossil *Globotruncana* (Abed and Ashur, 1987). Trace fossils are represented by *Thalassinoides* burrows. Phosphate, derived from marine fauna, was deposited as phosphate mud and then reworked and deposited as phosphate sands in shallow marine environment.

The **Umm Rijam Chert-Limestone Formation** (Eocene) is 220 m thick and consists of the alternation of chalky limestone, marly limestone and kerogenous limestone in its lower massive member and with appreciable amount of chert (beds and concretions) in its upper bedded member.

Tayyiba Limestone Formation consists of 2 informal members: a lower glauconitic and an upper 'cliffy' limestone. The lower glauconitic member consists of glauconitic sandstone, calcareous siltstone and marly limestone with shells of brachiopods and molluscs and tube-like fossils and trace fossils. The upper member consists of 3 cliffs of massive fossiliferous limestone. Nodular thinly bedded limestone is occasionally common at the base of these cliffs.

Clay mineralogy of the Belqa Group

Apart from Abed and Amireh (1985) and Shadfan et. al. (1985) there are no detailed studies on the clay mineralogy of the Belqa Group in north Jordan. The former authors reported that the clays constitute about 7% of the oil shale (bituminous marl) and are almost totally made of kaolinite with traces of illite, whereas the latter authors where the first to report palygorskite in the Umm Rijam Limestone. More detailed work has been carried out west of the Jordan River (Shoval, 2004). Illite/smectite is almost the only clay mineral except in the Danian Lower Taqiye Formatin where kaolinite is present. Palygoskite accompanies illite-smectite in the Ladenian Upper Taqiye and Lower Eocene Mor Formation. In the present work, clay mineralogy was not studied but the presence of clays is indicated by by alumina contents which, range from less than 1% to almost 11.74%.

Samples

16 representative samples from the dominant lithologies of the Late Cretaceous-Tertiary Belqa Group (Table 1) were collected at outcrop from Shallala (URC) and Wadi Tayiba (AHP and TL). These range from non-bituminous to slightly bituminous chalk, silicified chalk, marl, phosphorite, chert, glauconitic and fossiliferous limestone. The samples are summarized, along with their major oxides, in Table 2. Loss on ignition at 450°C reflects the organic matter content of the samples.

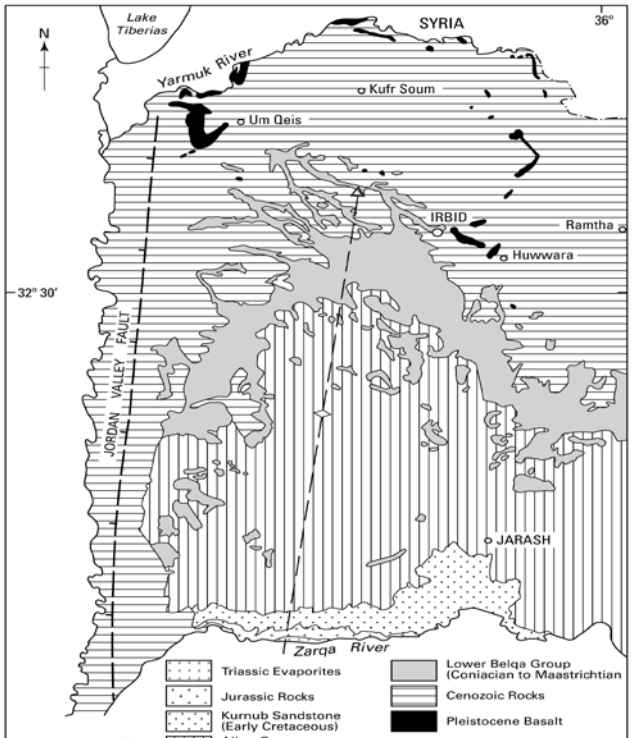

Figure 1 A simplified geological map of north Jordan. Study area is north of Irbid-Ramtha line (Abdelhamid et al., 1991).

Table 1. Stratigraphy of Belqa Group in the study area (Powell, 1989; Moh'd, 2000)

Age		Group	**Stage**	**Formation**	**Symbol**	**Main lithologies**
Tertiary (Neogene)		Belqa	Oligocene	Tayiba*	TL	Limestone, fossiliferous, glauconitic
			Eocene	Shallala	WSC	Chalk
				Umm Rijam*	URC	Chalk, chert, limestone
			Paleocene	Muwaqqar*	MCM	Chalk, marl, limestone concretions
Cretaceous	Late		Maastrichtian	Al Hisa*	AHP	Phosphorite, limestone, chert
			Santonian/ Campanian.	Amman	ASL	Chert, limestone, dolomite
			Coniacian	Umm Ghudran	WG	Chalk (massive and fossiliferous)
						Unconformity
	Early	Ajlun	Turonian	Wadi As Sir	WSL	Limestone, dolomite

*Units sampled for the present study

Analytical Procedures

Samples were analyzed using X-ray fluorescence (XRF) techniques at the Analytical Geochemistry Laboratories, British Geological Survey. In the present work oxides were analyzed using WD-XRFS fused glass beads, and most trace elements by WD-XRFS pressed powder pellets except Ag, Cd, In, Sn, Sb, Te, I, Cs, Ba, La and Ce which were analysed by ED(P)-XRFS pressed powder pellets. The samples were dried overnight at 105°C and pre-ignited with the temperature being ramped up from 200°C to 450°C, over the course of an hour and then for a further hour at 1050°C before analysis. Loss on ignition was determined after 1 hour at 1050° C and 1 hour at 450°C. Fe_2O_3t represents total iron expressed as Fe_2O_3. SO_3 represents sulphur retained in the fused bead after fusion at 1200C.

Results

The analytical results are presented in Tables 2 and 3. Correlation coefficients (r) between uranium and other analyzed elements are given in Table 4, and factor analysis is given in Table 5. The relationship between uranium and selected major and minor elements, and LOI are presented in cross-plots (Figures 2-12).

Table 2 Major oxides, LOI@450°C, and uranium concentration in the studied samples.

#	Lithology	Rock Unit	U ppm	SiO_2	Al+Fe	CaO+ LOI	MgO	P_2O_5	LOI@ 450°C
1	Slightly bituminous Chalk	URC	8	5.31	0.79	88.53	1.14	1.55	5.35
2	Slightly bituminous Marl	URC	6	23.39	15.14	58.17	0.93	1.11	1.87
3	Slightly bituminous silicified Chalk	URC	19	14.65	2.58	79.54	0.76	1.24	3.05
4	Slightly bituminous silicified Chalk	URC	12	13.92	3.40	74.52	2.3	0.30	5.49
5	Chalk	URC	4	2.64	0.94	95.59	0.40	0.96	0.86
6	Chalk	URC	4	2.81	0.86	94.96	0.40	0.93	0.95
7	Slightly silicified Chalk	URC	10	10.63	1.13	86.19	0.67	0.84	1.80
8	Limestone, fossiliferous	TL	<1	1.86	0.39	97.39	0.29	0.28	0.36
9	Slightly silicified Chalk	URC	11	8.66	1.45	87.00	0.80	0.93	1.52
10	Glauconitic Limestone	TL	10	6.26	3.48	86.60	0.78	2.27	0.65
11	silicified Chalk	URC	4	46.41	0.66	51.53	0.15	1.08	0.38
12	Chalk	URC	8	1.60	0.49	95.96	0.28	1.63	0.72
13	Phosphorite	AHP	70	1.83	0.46	81.00	0.35	14.49	1.16
14	Phosphorite	AHP	52	14.35	0.08	69.11	0.36	14.58	0.72
15	Chert	URC	2	95.32	0.16	3.77	0.05	0.26	1.95
16	Silicified Limestone	URC	4	64.51	0.43	34.00	0.08	0.55	1.96

Table 3. Average and standard error of the major, minor and trace elements.

	Average	Std error		Average	Std error		Average	Std error
SiO_2	19.63	6.67	Cl	1531.00	495.96	Sn	0.59	0.07
TiO_2	0.06	0.02	Sc	3.00	1.22	Sb	1.06	0.20
Al_2O_3	1.39	0.70	V	54.50	10.24	I	3.44	0.57
Fe_2O_3t	0.86	0.23	Cr	132.00	17.31	Cs	1.31	0.18
Mn_3O_4	0.01	0.00	Co	2.19	0.75	Ba	512.00	146.29
MgO	0.61	0.14	Ni	73.25	15.60	La	12.25	2.55
CaO	42.10	3.81	Cu	28.13	5.25	Ce	9.00	3.09
Na_2O	0.07	0.01	Zn	194.69	49.54	Nd	15.00	2.11
K_2O	0.10	0.04	Ga	2.06	0.75	Sm	3.06	0.06
P_2O_5	2.69	1.16	As	3.38	0.93	Cd	4.58	2.82
SO_3	0.46	0.13	Se	6.44	2.65	Yb	1.31	0.15
Cr_2O_3	0.02	0.00	Br	5.63	1.31	Hf	1.75	0.23
SrO	0.10	0.01	Rb	6.75	2.15	Ta	1.06	0.06
BaO	0.02	0.01	Sr	787.31	103.62	W	1.63	0.15
NiO	0.05	0.00	Y	22.75	3.87	Pb	1.94	0.62
ZnO	0.01	0.01	Zr	13.19	3.26	Bi	1.13	0.09
LOI	32.13	2.84	Nb	1.56	0.50	Th	1.38	0.26
Total	100.06	0.12	Mo	3.5	0.75	U	14.06	4.79
LOI@450	1.80	0.40	Ag	0.76	0.09			

Table 4 Correlation coefficients (r) between uranium and other components.

	r		r		r
SiO_2	-0.36	Cl	-0.12	Sn	0.63
TiO_2	0.15	Sc	0.83	Sb	-0.17
Al_2O_3	0.07	V	0.83	I	0.79
Fe_2O_3t	0.28	Cr	0.87	Cs	-0.13
Mn_3O_4	-0.08	Co	0.11	Ba	0.03
MgO	0.56	Ni	0.81	La	0.10
CaO	0.28	Cu	0.77	Ce	0.44
Na_2O	0.13	Zn	0.84	Nd	0.04
K_2O	0.38	Ga	0.09	Sm	0.35
P_2O_5	0.37	As	0.89	Cd	-0.08
SO_3	0.49	Se	0.63	Yb	0.22

Cr_2O_3	0.91	Br	0.71	Hf	0.14
SrO	0.50	Rb	0.42	Ta	-0.20
BaO	0.05	Sr	0.50	W	0.22
NiO	0.78	Y	0.66	Pb	0.06
ZnO	0.84	Zr	0.19	Bi	-0.12
LOI	0.35	Nb	-0.05	Th	0.03
Total	0.08	Mo	0.86		
LOI@450	0.46	Ag	0.18		

Table 5. Factor analysis, rotated component matrix, extracted by Principal Component Analysis.

	Factor 1	Factor 2	Factor 3
Explaining % variation	50.02	25.46	24.52
SiO_2	-0.657		-0.749
TiO_2	0.986		
Al_2O_3	0.988		
Fe_2O_3t	0.988		
MgO	0.976		
CaO	0.416		0.905
Na_2O	0.260	0.962	
K_2O	0.982		
P_2O_5	0.479		0.863
SO_3		0.988	
LOI	0.552		0.827
Total	0.402	0.478	0.781
LOI@450	0.365	0.537	-0.76
Cl	-0.364	0.932	
Sc	0.790	0.599	
V	0.955		0.292
Cr	0.595		0.768
Ni		0.977	
Cu	-0.276	0.960	
Zn	0.475	0.875	
Br	-0.427	0.887	
Rb	0.988		
Sr	0.283	0.318	0.905
Y	0.922		0.384
Zr	0.990		
I	-0.497		0.862
Ba	0.985		
Nd	0.984		
U	0.739	0.283	0.612

Uranium

The average uranium values in the samples is 14 ppm and the range is <1-70 ppm. Phosphatic samples (13 and 14) show a higher range (52-70 ppm). Other samples have a range from <1-19 ppm. Uranium is positively correlated with the following oxides: Cr_2O_3 (0.91), ZnO (0.84), and MgO (0.56). It also has positive correlation

with many trace elements. The strongest correlations being with As (0.89), Cr (0.87), Mo (0.86), Zn (0.84), V (0.83), Ni (0.81), and Sb (0.79).

U/SiO_2

SiO_2 shows a weak negative correlation (R=-0.36) with U (Figure 2). Figure 2 shows that the two phosphatic, as well as, siliceous samples (with SiO_2 >20%) have a linear inverse relationships with uranium with the former having higher gradient than the latter

(Uranium= -0.052 (SiO_2) + 6.9858 (R^2=0.94).

Of the siliceous samples in which uranium concentration is less than 10 ppm, chert has the lowest concentration of uranium, followed by silicified limestone, then siliceous chalks. On the other hand, pure and impure chalks (SiO_2<20%) have a positive relatively strong relationship with uranium (r>0.80) as follows:

Uranium= 0.8912 (SiO_2) + 2.6097 (R^2=0.75)

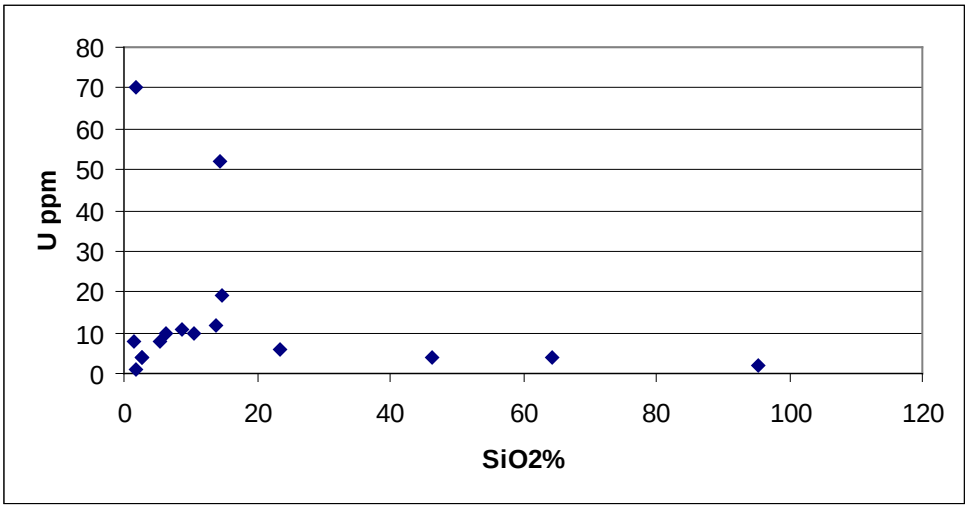

Figure 2. Correlation between U and SiO_2.

U/CaO

When CaO<35% (e.g. chert, silicified limestone, marl, highly siliceous chalk) uranium is less than 10 ppm. Non-phosphatic and low silica samples can be fit with a negative linear relationship as follows

Uranium= -0.819 (CaO) + 49.25 (R^2=0.64)

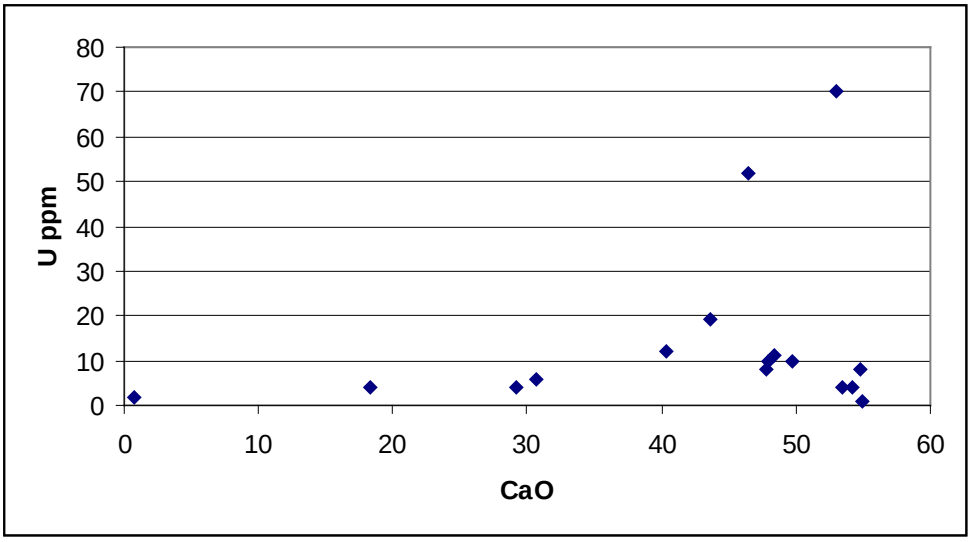

Figure 3. Correlation between U and CaO.

U/ P_2O_5

Uranium has a very strong positive relation with P_2O_5 (Figure 4) as shown in the following equation

$$\text{Uranium} = 791.67\ (P_2O_5) + 35.75 \quad (R^2 = 0.92)$$

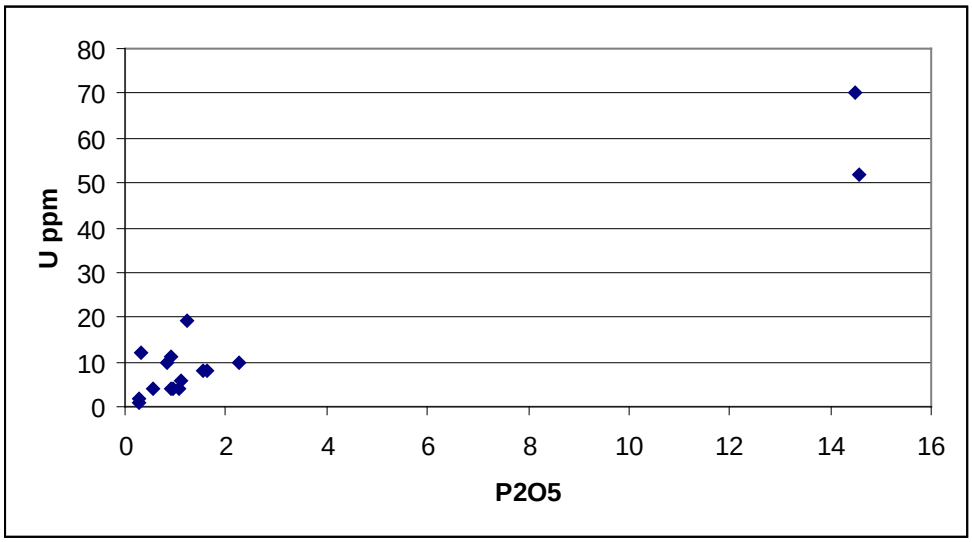

Figure 4. Correlation between U and P_2O_5.

U/ Cr

The positive high correlation coefficient (r=0.87) between uranium and Cr is shown in Figure 5. The figure consists of two almost parallel separate lines. When taken separately, the upper line represents phosphorites

$$\text{Uranium} = 0.261\ (\text{Cr}) + 34.78\ (R^2 = 1.00)$$

The lower line represents the rest of the samples

$$\text{Uranium} = 0.058\ (\text{Cr}) - 0.56\ (R^2 = 0.92)$$

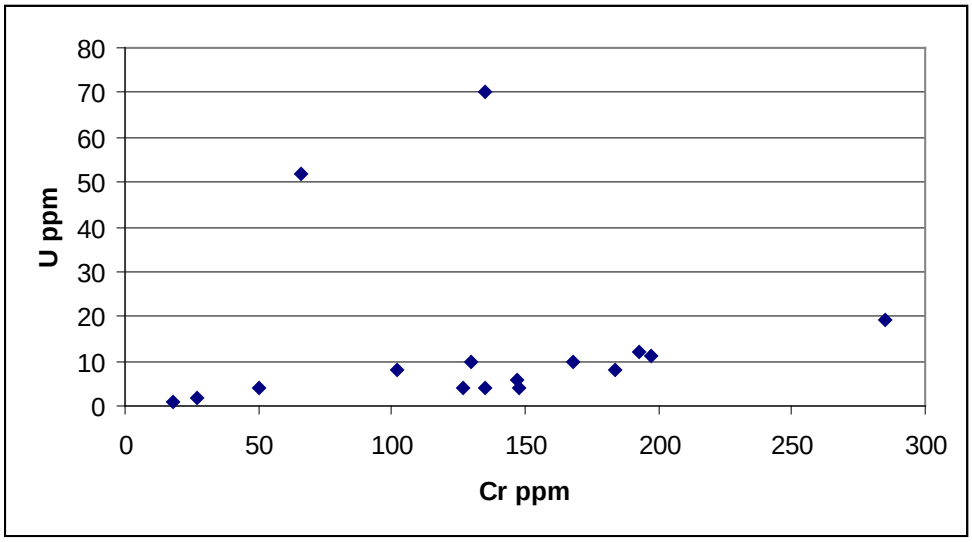

Figure 5: Correlation between U and Cr.

U/SrO

The best fit between uranium and SrO and including all samples (Figure 6) is an exponential one as shown in the following equation

$$\text{uranium} = 1.699\ e^{14.84\ (\text{SrO})}$$

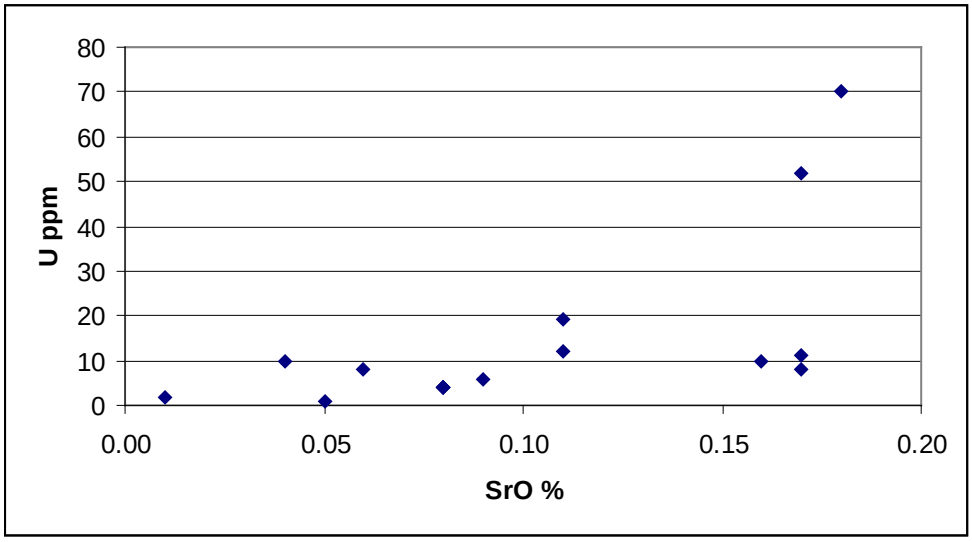

Figure 6: Correlation between U and SrO.

U/Zn

Zn (Figure 7) has positive linear relations with uranium when phosphatic samples are excluded.

$$\text{Uranium} = 0.026\ Zn + 3.33 \quad (R^2 = 0.70)$$

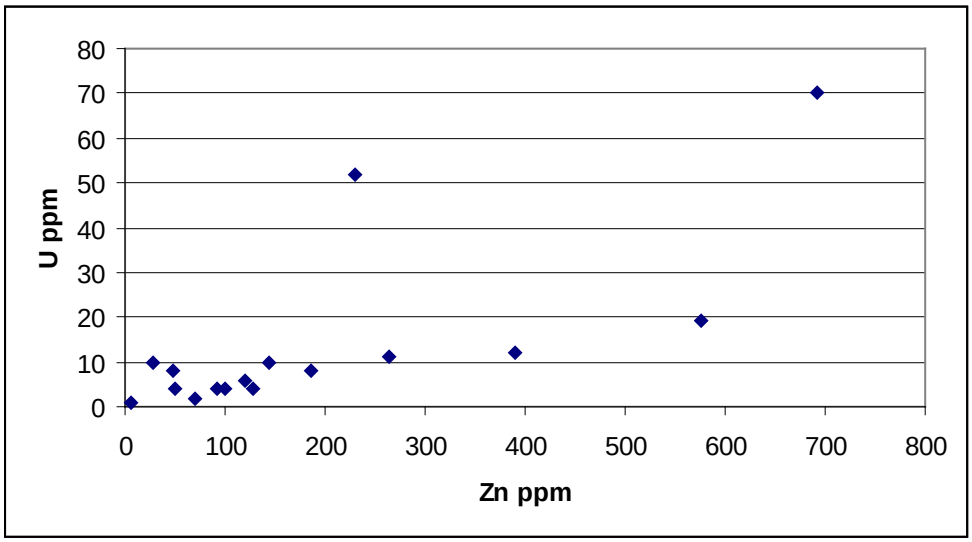

Figure 7: Correlation between U and Zn.

U/V

Vanadium (Figure 8) has a strong positive linear relationship with uranium when phosphate samples are excluded. This relationship has the following equation

$$\text{Uranium} = 0.099\ V + 2.48 \quad (R^2 = 0.70)$$

Uranium and vanadium are characteristically negatively related in the phosphate samples

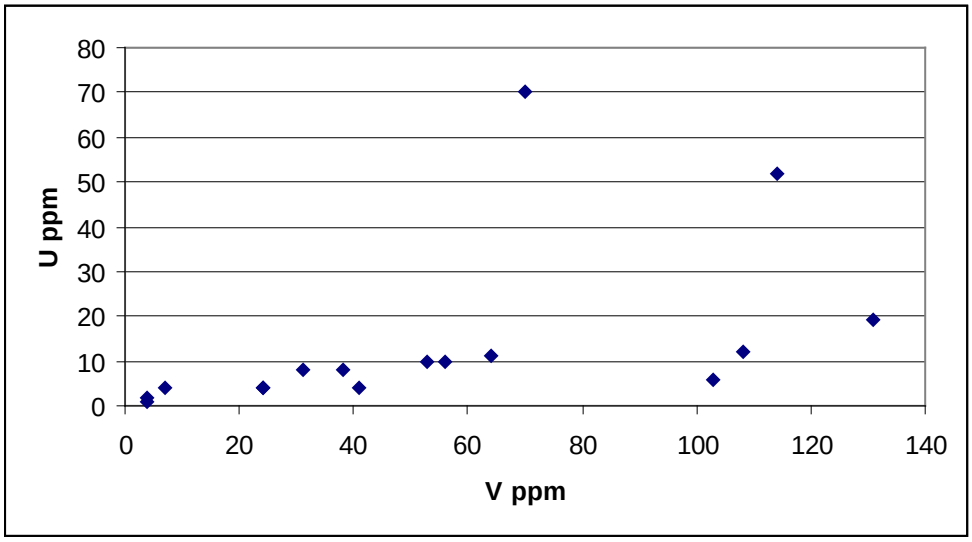

Figure 8: Correlation between U and V.

U/Mo

Mo (Figure 9) has also a positive linear relationship with uranium when phosphates are excluded. This relationship has the following equation

Uranium= 1.255 Mo + 3.144 (R^2=0.74)

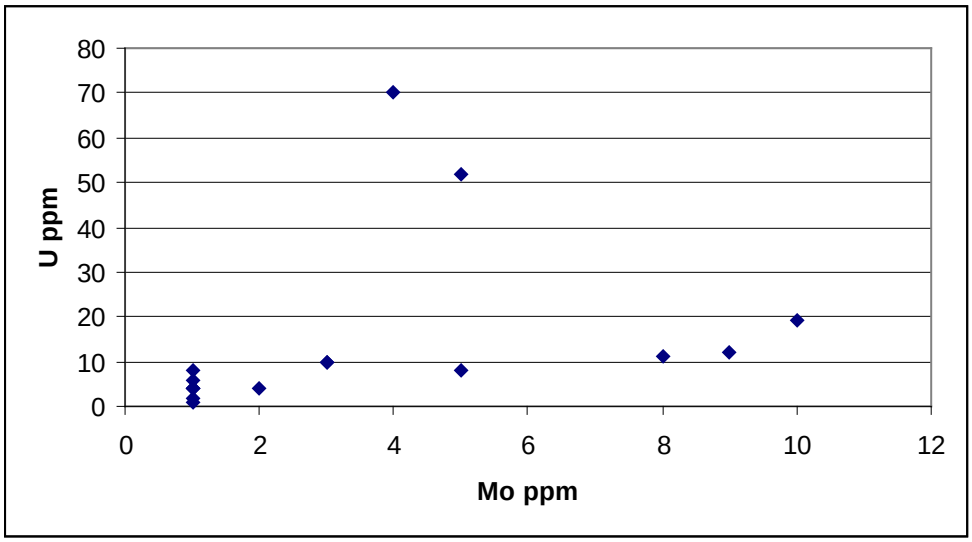

Figure 9. Correlation between U and Mo.

U/Loss on Ignition (LOI)

Three straight lines can fit the LOI (Figure 10) in the different samples with uranium. The first line being with phosphate samples where a positive relationship with

uranium is evident. The second line includes chert, silicified limestone, highly siliceous chalk and marl which show a positive linear relationship

$$\text{Uranium} = 0.1455\ \text{LOI} + 1.51 \qquad (R^2 = 0.89)$$

The rest of the samples show a negative relationship with uranium as shown in the following equation

$$\text{Uranium} = -2.011\ \text{LOI} + 88.13 \qquad (R^2 = 0.81)$$

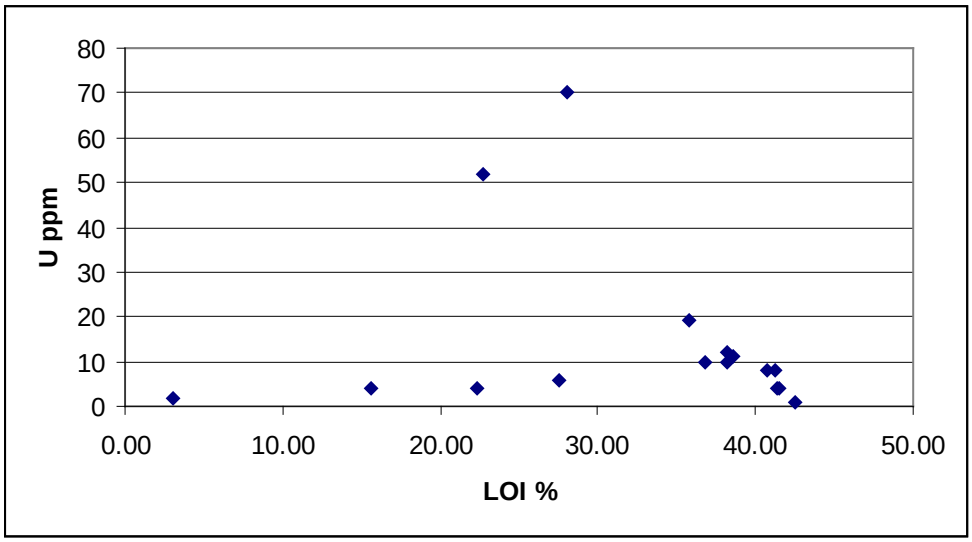

Figure 10: Correlation between U and LOI.

An approximate estimate of uranium content can be derived from the knowledge of the total chemical analysis (including all oxides and LOI) (Figure 11) using the following equation

$$\text{Uranium} = -30.4\ \text{Total} + 3056.2 \qquad (R^2 = 0.57)$$

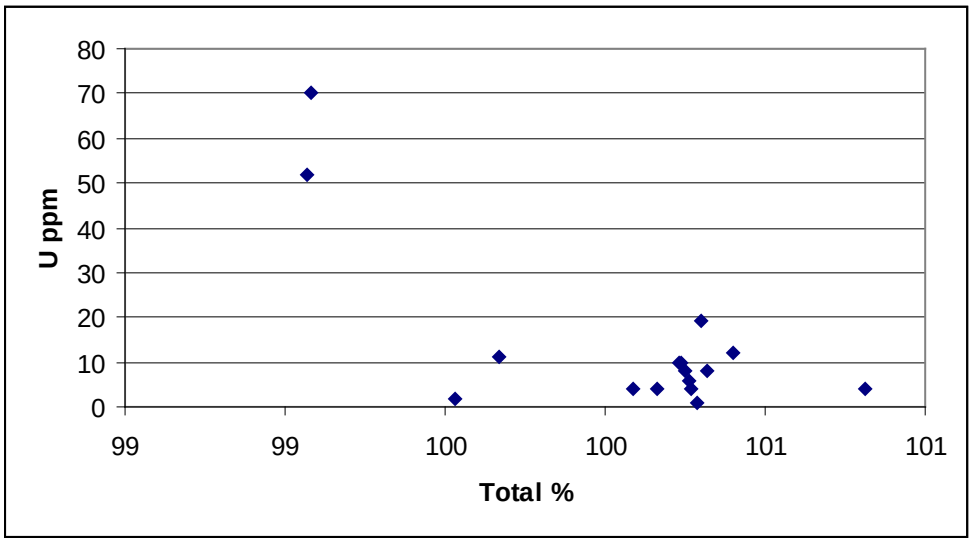

Figure 11 Correlation between U and total components.

LOI@450C is related to carbonates, organic matter and clay minerals and shows at least three trends or fields with uranium. The first is a negative trend that includes slightly bituminous samples. The second trend is also negative and includes chert, silicified limestone, marl and highly siliceous chalks. The third field includes the rest of samples.

Discussion

Uranium in Late Cretaceous to Early Tertiary rocks (Jordan)

Turekian and Wedepohl (1961) reported the following average uranium concentrations (in ppm) in the main types of sedimentary rocks: shale 3.7, sandstone 0.45 and limestone 2.2. These compare with 2.7 ppm in igneous rocks. In non-bituminous Upper Cretaceous chalk of the United States, Gale et. al., (2008) reported less than 2 ppm of uranium. Similarly, Kuzendorf and Sorensy (1989) and Stemmerik et. al. (2006), reported concentrations of less than 2 ppm for Upper Cretaceous chalks of the North Sea and of Stvens Klint, Denmark. However, along the southern margin of the Late Cretaceous to Neogene Tethys Ocean uranium concentrations are higher. For instance, Ilani et al (2006) reported the following figures for U concentrations from formations penetrated by a well drilled in the vicinity of the western shores of Tiberia lake: 4.6 ppm from Timrat (Eocene), 8.9 ppm from Taqiya (=Muwaqqar Chalk Marl, in part), 5.5ppm from Ghareb (=Muwaqqar Chalk Marl, in part), and 8-23.6ppm from En Zetim (=Umm Ghudran to Al Hisa Phosphorite), with high concentrations being associated with oil shale horizons. Furthermore, Late Cretaceous to Neogene shallow marine phosphorites in the Tethyan belt including Egypt and the Levant, commonly have high uranium contents compared to the world average for phosphates (120 ppm; Altschuler, 1980). Uranium contents of 90-150 ppm of U have been reported in Negev Phosphorites (Nathan et. al, 1979; Gross and Ilani, 1987; Gill and Shiloni, 1995) and 50-357 ppm in Egypt (El-Arabi and Khalifa, 2002). Uranium content in the economic Cretaceous to Neogene phosphorite belt of Jordan ranges from 65 -170 ppm (Abu Ajamieh et al, 1988; Smith et al., 1996b).

Uranium in the Upper Cretaceous to Lower Tertiary oil shales was first reported from the Lajjun deposit in central Jordan by Hufnagel et. al. (1980) as 26 and 24 ppm in Boreholes 86 and 97, respectively. More recent work on oil shale of Jordan has been carried out by Abu Murad (2008) who reported the following uranium concentrations from oilshale deposits in central Jordan: Lajjun 31.4, Sultani 12.3, Jurf 9.8, Attarat 16.7, Wadi Maghar 12.5, Siwaqa 9.7, Khan Az-Zabib 28.1, and Eth Thamad 41.6 ppm.

The analytical results (Tables 2-3) and statistical analysis (Tables 4-5, and Figures 2-12) from this study demonstrate the close association of U with other major and minor elements in Late Cretaceous to Early Tertiary samples (full analytical results, not included for brevity, are available for the authors). Uranium is most strongly associated with phosphorite deposits where the metal is present together with other trace elements in the phosphate mineral francolite $Ca_5(CO_3\ P0_4)_3(F,OH)$ lattice where U partially substitutes for calcium in the mineral lattice (McClellan and Van Kauwenbergh, 1990; Wriekat et al., 1987). A positive correlation between uranium

and phosphorite deposits has been recognized in the region (Gill and Shiloni, 1995; Abed and Khaled, 1985). In Jordan, the Late Cretaceous Campanian to Maastrichtian phosphorite belt shows a general decrease from north to south in the mean concentration of both phosphate and associated uranium from the Zarqa (Ruseifa) area, immediately south of the study area, (29.7% P_2O_5; 145 U ppm) to Esh Shidiya (24.85% P_2O_5; 80 U ppm (Saadi and Shaban, 1981; Smith et al, 1996b). This trend is attributed to a southward decrease in the purity of the phosphate rock, and hence in the proportion of uranium substituting in the francolite lattice. The relatively low U content (52-70 ppm) in the samples analyzed in this study from northwest Jordan indicate a lower phosphate, and hence uranium, content. This trend is attributed to the palaeoenvironmental setting of the studied rocks in more basinal (offshore) locations during deposition of the Belqa Group sediments on a pelagic ramp at the southern margin of the Tethys Ocean (Powell, 1989).

The presence of U contents ranging from 8 ppm to 19 ppm in chalk lithologies from Umm Rijam Chert-Limestone reflects the presence of uranium in slightly bituminous chalks. The organic matter in these chalks is associated with minor amounts of similar organic fish and marine vertebrate fragments that make up much of the original source of francolite in these phosphorite lithologies. A similar relationship can be seen in the higher than average phosphate and uranium concentrations in the marine glauconitic marl from the Oligocene Tayiba Formation (Table 2).

Trace metals such as Mo, Zn,V, Ni, Cr, As and Mo have strong ($r>0.80$) positive correlation with uranium, and are mostly associated with organic matter (bitumen and francolite).

Factor analysis (Table 5) resulted in deriving 3 factors explaining 100% of the variations of the data. Factor 1 explains 50% of the data variation and is controlled by clay minerals, and to less extent, by carbonate. Factor 2, explaining 25% of the variation, is controlled by both depositional/diagenetic water and organic matter content. Factor 3, explaining also 25% of the variation, is controlled by phosphorite beds. Uranium was found to be associated with the three factors but with different loadings. Association of uranium with factor 2 (organic matter and ground water) is weak in comparison to association with factors 1 and 3.

Conclusions

Uranium concentrations in Jordanian Late Cretaceous to Tertiary (Neogene) chalks are higher than those of the standard limestone and equivalent ‘pure’ chalk (98% $CaCO_3$) of USA and northwest Europe. High uranium concentrations are closely associated with phosphorite deposits, in which uranium substitutes for calcium in the francolite lattice. Higher than average levels of uranium, in slightly bituminous chalks and glauconitic limestones are attributed to minor amounts of organic matter found in these samples.

Uranium association with organic matter and formation water is weak in comparison to association with the clays and carbonates (factor 1), and P_2O_5 (factor 3). Trace elements (Cr, Mo, Zn, V, Ni, Cl, As, and Mo) have strong positive relations with Uranium (with $r>0.80$).

The correlation matrix should not be relied upon totally as it gives average correlation coefficients (assuming linear relationships between variables) when dealing with different lithologies. Cross-plotting results may emphasize the effect of different lithologies and different curves may be used to fit the data. Cross-plotting may reveal relationships with lithologies that are not clear in the correlation matrix.
Exploration for uraniferous deposits of economic value should be focused on phosphorite and/or associated phosphorite/high bituminous sedimentary rocks, especially where these lithofacies reach high levels of P_2O_5 in the Late Cretaceous to Neogene Tethyan phosphorite belt.

Acknowledgements

The authors thank Charles Gowland and Mark Ingham of the BGS Analytical Laboratories for chemical analyses and discussion of the results. BKM would like to thank Tafila Technical University for a travel grant to the UK during 2008 summer. JHP publishes with permission of the Executive Director, British Geological Survey (NERC).

References

Abdelhamid, G., Moh'd, B., and Barjous, M.,1991, The geology of northwest Jordan 'to accompany the preliminary 1: 100 000 geological map', *Internal Report*, Amman.

Abed, A., and Amireh, B., 1983, Petrography and geochemistry of some Jordanian oil shales from north Jordan. *Journal of Petroleum Geology*, **5**(3): 261-274.

Abed, A., and Khaled, H., 1985, Uranium in Esh-Shediya phosphates, *Dirasat* **8**: 57-66.

Abu Ajamieh, M., 1974, Uranium in the Jordanian phosphates, *Unpublished Report*, Natural Resources Authority, Amman, Jordan.

Abu Ajamieh, M., 1981, Radioactive minerals in Jordan, *The 4TH Arab Mineral Resources Conference*, Amman, 2: 16p.

Abu Ajamieh, M., 1987, Mineral resources of Jordan, *Unpublished Report*, Natural Resources Authority, Amman, Jordan.

Abu Ajamieh, M., Bender, F.K. and Eicher, R. N. 1988. *Natural Resources in Jordan*, pp. 224. Natural Resources Authority, Amman, Jordan.

Abu Murad, K., 2008, Determination of uranium concentration in Jordanian oil shale using fission fragments technique with cx-39, 24th International Conference on Nuclear Tracks in solids, 1-5 Sep., 2008, Bologna, Italy.

Altschuler, Z.S. 1980. The geochemistry of trace elements in marine phosphorites, Part 1: Characteristic abundances and enrichment. *SEPM Special Publication* , **575-B**, 19-30.

El-Arabi, A.M. and Khalifa, I.H., 2002. Application of multivariate statistical analyses in the interpretation of geochemical behaviour of uranium in phosphatic rocks in the Red Sea, Nile Valley and Western desert, Egypt. *Journal of Environmental Radioactivity,* **61**, 169-190.

Gale, A., Hancock, J., Kennedy, W., Petrizzo, M., Lees, J., Ireneusz Walaszczyk, I., and Wray, D. 2008, An integrated study (geochemistry, stable oxygen and carbon isotopes, nannofossils, planktonic foraminifera, inoceramid bivalves, ammonites and crinoids) of the Waxahachie Dam Spillway section, north Texas: a possible boundary stratotype for the base of the Campanian Stage, Cretaceous Research 29: 131-167.

Healy, R. and Young, J. 1998, Mineralogy of U-bearing marls from the Jordanian Desert, Unpublished Report for Cameco Corporation, Canada.

Gill, D., and Shiloni, Y. 1995. Abundance and distribution of uranium in Senonian phosphorites, Arad basin, southern Israel. *Journal of African Earth Sciences* , **20**, 17-28.

Gross, S., and Ilani, S. 1987. Secondary uranium minerals from the Judean Desert and northern Negev, Isreal. *Uranium*, **4**, 147-158.

Helmdach, F., Khoury, H., and Meyer, J. 1985, Secondary uranium mineralization in the Santonian-Turonian, near Zarqa, north Jordan, *Dirasat*, **12**: 105-111.

Hufnagel, H., Schmitz, H., and El-Kaysi, K., 1980, Investigation of the El-Lajjun oil shale deposit, Technical Cooperation Project No. 78.2165.5, Bundesanstalt fur Geowissen-Schaften und Rohstoffe, Hannover, Germany.

Ilani, S., Minster, T., Kronfeld, J., and Even, O., 2006, The source of anomalous radioactivity in the springs bordering the Sea of Galilee, Israel, *Journal of Environmental Radioactivity,* **85**: 137-145.

Kunzendorf, H. and Sorensey, P., 1989, Geochemical criteria for reservoir quality variations in chalk from North Sea, Riso National Laboratory, Roskilde, Denmark, 99p.

McClellan, G.H. and Van Kauwenbergh, S.J. 1990. Mineralogy of sedimentary apatites. In: Phosphorite Research and Development, Notholt, A.J.G. and Jarvis, I. Eds. *Geological Society Special Publication,* **52**, 23-31.

Moh'd, B., K., 2000, The geology of Irbid and Ash Shuna Ash Shamaliyya (Waqqas) map sheets, *Geology Directorate, Bulletin* **46**, Natural Resources Authority, Amman, Jordan .

Nathan, Y., Shiloni, Y., Roded, R., Gal, I., and Deutch, Y., 1979, The geochemistry of the northern and central Negev phosphorites, *Israel Geological Survey Bulletin* 73: 41p.

NRA, 1997, Uranium exploration in Siwaqa area, Unpublished Report, in Arabic.

Phoenix Corp., 1980, A comprehensive airborne magnetic /radiation survey of the Hashemite Kingdom of Jordan, Internal Report, NRA, Amman.

Powell, J H. 1989. Stratigraphy and sedimentation of the Phanerozoic rocks in central and southern Jordan. *Bulletin 11, Geology Directorate, Natural Resources Authority (Ministry of Energy and Mineral Resources) Amman, H K of Jordan.* Part B : Kurnub, Ajlun and Belqa Groups, 161pp, 12 figs., 17 tables.

Saadi T.A. and Shaban, M.R.1981. *Arab Mining Journal*, **1**, 70-70.

Shadfan, H., Dixon, J., and Kippenber, L., 1985, Palygorskite distribution in Tertiary limestone and associated soils of northern Jordan. *Soil Science*140 (3): 206-212.

Shoval, S., 2004, Clay sedimentation along the southeastern neo-Tethys margin during the oceanic convergence stage, *Applied Clay Science* 24: 287-298.

Smith, B, Powell, J H, Bradley, A D, Gedeon, R, and Amro, H. 1995. Naturally occurring uranium pollution in Jordan. *Mining Environmental Management,* **3**, 7-10.

Smith, B, Powell, J H, Gedeon, R, and Amro, H. 1996a. Radiological and chemical hazards associated with natural series radionuclides in the Amman-Zarqa basin, Jordan: a case study. 449-464, In: *6th Spanish Congress and International Conference on Environmental Geology and Land-Use Planning, Natural Hazards, Land-use Planning and Environment*, Vol. III, Chacon, J and Irigaray, C (eds).

Smith, B, Powell, J H, Gedeon, R, and Amro, H. 1996b. Groundwater pollution by natural radionuclides: an evaluation of natural and mining contamination associated with phosphorite (Jordan). 375-394, In: *Minerals, Metals and the Environment II*, Prague. Conference Proceedings. Institution of Mining and Metallurgy, London.

Smith, B, Hutchins, M.G., Powell, J H, Talbot D, Trick, J K, Gedeon, R, Amro, H, Kilani, S, Constantinou, G, Afrodisis, S, and Constantinou, C. 1997. The distribution of natural radioelements in groundwaters and Cretaceous-Neogene sediments from the south-east Mediterranean region. *Presented at the 4th International Environmental Geochemistry Symposium, Vail, Colorado*, Oct. 1997.

Stemmerik, L., Surlyk, F., Klitten, K., Rasmussen, L., and Schovsbo, N., 2006, Shallow core drilling of the Upper Cretaceous chalk at Stevns Klint, Denmark, *GEUS Geological Society of Denmark and Greenland Bulletin* **10**: 13-16.

Turekian, K. and Wedepohl, K., 1961, Distribution of the elements in some major units of the earth crust, *Geological Society American Bulletin* **72**: 175-192.

Wriekat, A., Abdullah, M., and Saffarini, G., 1987, The determination of U and Th in some Jordanian mineral deposits using natural gamma ray spectroscopy, *Dirasat* **14**: 187-191.